Energy Efficient Analog Beamformer Design for mmWave Multicast Transmission

Zihuan Wang, *Student Member, IEEE*, Qian Liu, *Member, IEEE*, Ming Li, *Senior Member, IEEE*, and Wolfgang Kellerer, *Senior Memeber, IEEE*

***Abstract*—Millimeter wave (mmWave) communication is considered as a key enabling technology for 5G cellular networks because abundant spectrum in mmWave bands can provide multi-gigabit communication service. Analog beamforming architecture, which employs energy-efficient phase shifters (PSs) instead of energy-hungry radio frequency (RF) components, has emerged as a promising solution to overcome severe propagation loss of mmWave channels. On the other hand, multicast communication is another efficient approach to address the dramatic traffic demand by utilizing the broadcast nature of the wireless medium. This paper investigates energy efficient analog beamforming in mmWave single-group multicast communication systems. We focus on max–min fair (MMF) problem and aim to design the analog beamformer to maximize the minimum signal-to-noise ratio (SNR) over all users subject to a transmit power constraint. The analog beamformer design with infinite and finite resolution PSs are both studied. While the constraints of PSs make the problem intractable, we propose an alternative low-complexity algorithm, which iteratively determines each element of analog beamformer. Furthermore, we also investigate the asymptotically optimal beamformer designs and provide asymptotic performance analysis for large-scale mmWave multicasting systems. Extensive simulation results illustrate the effectiveness of the proposed analog beamforming designs in mmWave multicast systems. Besides, numerical results also demonstrate that the asymptotic performance of the proposed scheme is close to the optimal case.**

***Index Terms*—Millimeter wave communication, analog beamforming, multicasting, energy efficiency, phase shifter.**

I. Introduction

BECAUSE of the substantial traffic growth driven by emerging applications, such as virtual and augmented realities, ultra-high definition video, high transmission rate has become one of the most important features in the fifth-generation (5G) and beyond wireless communication systems. Millimeter wave (mmWave) communication combined with large-scale antenna arrays is a key technology for 5G mobile communications because it can dramatically improve the data rates and achieve enormous transmission capacity [2]–[4]. Meanwhile, another important attribute of 5G systems for real-world implementation is energy efficiency since green communication has become an irresistible trend [5]. Conventional full-digital beamforming, which requires large number of radio frequency (RF chains, will result in high energy consumption and hardware cost, and is impractical for mmWave communication systems [6], [7]. Therefore, efficient analog beamforming architectures have been widely considered for mmWave systems, which can significantly reduce the energy consumption and cost while maintaining acceptable signal-to-noise ratio (SNR) of transmission links.

In analog beamforming architectures, a single RF chain is connected to a large number of energy-efficient and economical phase shifters (PSs). The analog beamformers are implemented at RF domain which can provide sufficient beamforming gain for mmWave transmissions [6]. Note that the power consumed by a PS is at the level of several to tens of milliwatts, while an RF chain consumes several hundred milliwatts [7]. Thus, analog beamforming can dramatically reduce power consumption while generate sufficient beamforming gain, and has drawn significant interest in both industry and academia [8]–[11]. Later on, in an effort to implement multiplexing/multiuser transmission, analog/digital hybrid beamforming architecture is proposed, which requires a few number of RF chains to realize a low-dimension digital beamformer and combines it with the high-dimension analog beamformer [12]–[15].

On the other hand, with the proliferation of streaming media and large-scale software updates, it is expected that the spectral efficiency of wireless communications can be improved by serving multiple users simultaneously, which facilitates the revival of interest in physical layer multicasting [16]. With the aid of multi-antenna techniques, multicast beamforming can simultaneously deliver common messages to a group of users, which efficiently addresses the significant traffic demands as well as saves spectrum resources. Obviously, combining multicast transmission with mmWave analog beamforming is becoming an important research trend to further improve both the energy efficiency and the spectral efficiency.

Manuscript received September 15, 2018; revised February 3, 2019; accepted April 2, 2019. Date of publication April 11, 2019; date of current version May 16, 2019. This work was supported in part by the National Natural Science Foundation of China under Grant 61671101, Grant 61601080, and Grant 61761136019. Part of this work will be presented at IEEE Vehicular Technology Conference (VTC), Kuala Lumpur, Malaysia, April 2019 [1]. The associate editor coordinating the review of this paper and approving it for publication was X. Zhang. *(Corresponding author: Ming Li.)*

Z. Wang and M. Li are with the School of Information and Communication Engineering, Dalian University of Technology, Dalian 116024, China (e-mail: wangzihuan@mail.dlut.edu.cn; mli@dlut.edu.cn).

Q. Liu is with the School of Computer Science and Technology, Dalian University of Technology, Dalian 116024, China (e-mail: qianliu@dlut.edu.cn).

W. Kellerer is with the Department of Electrical and Computer Engineering, Technical University of Munich, 80290 Munich, Germany (e-mail: wolfgang.kellerer@tum.de).

Digital Object Identifier 10.1109/TGCN.2019.2910316

A. Prior Work

Analog and hybrid beamformer designs have been widely studied in recent years. The major challenge of the analog and hybrid beamformer designs lies in the constant magnitude constraint of the analog beamformer, which is imposed by PSs. For the case that PSs have continuous phase (i.e., infinite resolution), the most popular solution is to transform the original spectral efficiency maximization problem to minimizing the Euclidean distance between the analog/hybrid beamformers and the full-digital unconstrained beamformer [17]–[19]. Besides, some other successive design approaches are also proposed to directly maximize the spectral efficiency [20], [21]. In [22], the authors propose an iterative algorithm to design the hybrid beamformer, which is shown to achieve performance very close to the full-digital case.

Though those infinite resolution PSs based analog beamformer designs can achieve near-optimal performance in mmWave communication systems, discrete phase (i.e., finite resolution) PSs are generally employed in practical systems because low resolution PSs are easier to be realized and more energy-efficient. For discrete phase analog beamformer design, a simple approach is to firstly obtain the optimal continuous phase analog beamformer, and then directly quantize the phase of each element to a finite set [22]–[24]. In addition, the discrete phase analog beamformer can be obtained by searching over a pre-designed codebook [8], [9], [25]–[27], or based on a machine learning approach [28].

While the analog and hybrid beamformer designs for mmWave point-to-point or downlink multiuser systems have been intensively studied, hybrid beamforming in mmWave multicast systems has not been well investigated. The multicast beamformer designs are generally formulated as *i*) the quality of service (QoS) problem which aims at minimizing the transmit power under the prescribed SNR constraint of each user, or *ii*) the max-min fair (MMF) problem that attempts to maximize the minimum SNR of all users under a total power constraint. In conventional full-digital beamforming systems, the multicast beamformer design is usually a non-convex quadratically constrained quadratic programming (QCQP) problem, which can be solved by the classic semi-definite relaxation (SDR) approach [16], [29], or fast algorithms such as successive convex approximation (SCA) [30] and alternating direction method of multipliers (ADMM) [31]. With regard to hybrid multicast beamforming, the authors in [32] proposed a beam searching algorithm to determine the analog beamformer, followed by the traditional SDR method to compute the digital beamformer. Unfortunately, the proposed beamformer searching procedure is still of high complexity. In [33], the hybrid multicast beamforming using two-bit resolution PSs was considered. While the proposed solution can significantly reduce the power consumption and hardware complexity, the performance will degrade when the number of RF chains is not sufficient large. The authors in [34] proposed to alternatively optimize the analog and digital beamformers based on concave-convex procedure (CCP), which can achieve the same performance as SDR-based full-digital case. However, the analog beamformer is assumed to be realized by vector modulator that can continuously adjust the phase and magnitude of the RF signals, which seems impractical for mmWave communication systems.

Overall, the aforementioned beamformer designs are all based on the hybrid beamforming architectures, which require multiple energy-intensive RF chains and have relatively high power consumption. Therefore, pure analog beamforming utilizing only one RF chain, is highly desired for mmWave multicast communication because of its significant advantage on energy efficiency.

B. Contributions

In this paper, we investigate the MMF problem in a single-group mmWave multiple-input single-output (MISO) multicasting system and aim to design the analog beamformer to maximize the minimum SNR of all users under a total power constraint. To the best of our knowledge, the analog beamformer design for mmWave multicast systems has not been studied before. The contributions of this paper come from two aspects.

We consider the analog beamformer design with infinite and finite resolution PSs, respectively, to maximize the minimum received SNR among users in mmWave systems. While the constraints of PSs make the problem intractable, we alternatively seek a near-optimal solution with low-complexity while achieving satisfactory performance. In particular, we reformulate a sub-optimal objective function and iteratively determine each element of analog beamformer. It is shown that our proposed algorithm can achieve close performance to the full-digital case with low-complexity and enjoys significant advantage in terms of energy efficiency.

We also study the asymptotic performance of mmWave multicast beamforming systems with very large-scale antenna arrays. Note that conventional beamformer designs may be not feasible in this case since the complexities increase with the number of antennas, and a fast approach is desired. Based on the asymptotic characteristic of mmWave channels, we can easily obtain the closed-form of asymptotically optimal full-digital beamformer, which is served as the foundation for analog beamformer design. Then, for the analog beamforming systems, we propose a simple asymptotically optimal design by directly normalizing and quantizing each element of the asymptotically optimal full-digital beamformer. The asymptotic performance lower-bounds of the proposed analog designs are also presented for evaluating the achievable SNR of mmWave multicasting systems with large-scale antenna arrays.

C. Organization and Notations

The rest of the paper is organized as follows. Section II introduces the system model of mmWave multicasting system and presents the MMF problem formulation. Section III specifies the proposed analog beamformer designs based on infinite and finite resolution PSs, respectively. After providing the asymptotic performance analysis in Section IV, simulation results are shown in Section V. Finally, we draw our conclusions in Section VI.

The following notations are used throughout this paper. Boldface lower-case and upper-case letters indicate column

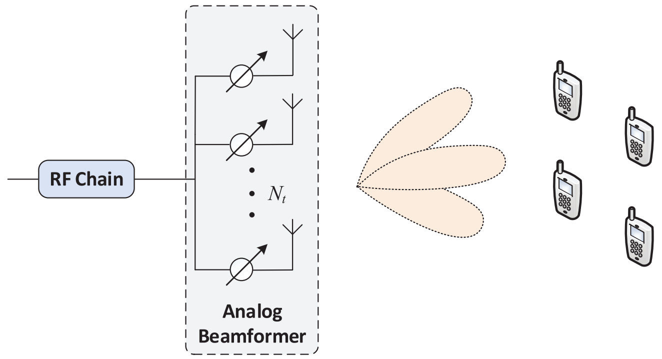

Fig. 1. A typical mmWave multicast transmission system with analog transmit beamformer.

vectors and matrices, respectively. $(\cdot)^*$, $(\cdot)^T$, and $(\cdot)^H$ denote the conjugate, transpose, and conjugate-transpose operations, respectively. $\angle a$ denotes the angle of complex number a. $\mathbb{E}\{\cdot\}$ represents statistical expectation. $\mathbb{C}$ and $\mathbb{R}$ denote the sets of complex numbers and real numbers, respectively. $|\mathcal{A}|$ is the cardinality of set $\mathcal{A}$. $|a|$ and $\|\mathbf{a}\|$ are the magnitude and norm of a scalar a and vector $\mathbf{a}$, respectively. Finally, we adopt a MATLAB-like matrix indexing notation: $\mathbf{a}(i)$ denotes the i-th element of vector $\mathbf{a}$.

II. System Model and Problem Formulation

A. System Model

We consider a single-group mmWave multicasting system with analog transmit beamforming at the base station (BS), as illustrated in Fig. 1. The BS employs N_t antennas and a single RF chain to simultaneously serve K users. Since implementing beamforming should be very challenging at the user side due to high hardware cost and power consumption, we assume each user is equipped with a single antenna. The transmitted signal is precoded with an analog beamformer $\mathbf{f}_{RF}$. Because the analog beamformer $\mathbf{f}_{RF}$ is implemented by a PS network, each element of $\mathbf{f}_{RF}$ has a constant amplitude, i.e., $|\mathbf{f}_{RF}(i)| = \sqrt{\frac{P}{N_t}}, \forall i = 1, \ldots, N_t$, where P is the total transmitted power. Let $\mathbf{h}_k \in \mathbb{C}^{N_t \times 1}$ denote the mmWave channel vector from the BS to the k-th user. Then, the received signal at the k-th user can be expressed as

$$y_k = \mathbf{h}_k^H \mathbf{f}_{RF} s + n_k, \ k = 1, \ldots, K, \tag{1}$$

where s is the transmitted symbol, $\mathbb{E}\{|s|^2\} = 1$, $n_k \sim \mathcal{CN}(0, \sigma_k^2)$ is the complex Gaussian noise vector corrupting the received signal. Then, the SNR of each user can be expressed as

$$\mathrm{SNR}_k = \frac{\left|\mathbf{h}_k^H \mathbf{f}_{RF}\right|^2}{\sigma_k^2}, \ k = 1, \ldots, K. \tag{2}$$

In this paper, the typical far-field line-of-sight propagation is considered and the channel vector of the k-th user is formulated as [25]

$$\mathbf{h}_k = \sqrt{N_t}\alpha_k \mathbf{a}_t(\theta_k), \tag{3}$$

where α_k is the complex gain of the propagation path (ray) and $\theta_k \in [-\frac{\pi}{2}, \frac{\pi}{2}]$ is the angle of departure (AoD), which is assumed to follow uniform distribution. $\mathbf{a}_t(\theta_k)$ is the beam steering vector, which only depends on antenna array structures. When the commonly used uniform linear array (ULA) is considered, the beam steering vector can be expressed as

$$\mathbf{a}_t(\theta_k) = \frac{1}{\sqrt{N_t}}\left[1, e^{j\frac{2\pi}{\lambda} d \sin(\theta_k)}, \ldots, e^{j(N_t-1)\frac{2\pi}{\lambda} d \sin(\theta_k)}\right]^T, \tag{4}$$

where λ is the signal wavelength, and d is the distance between antenna elements. In this paper, we assume the knowledge of $\mathbf{h}_k$ of each user is known at the BS, which can be obtained by efficient channel estimation algorithms [7].

B. Max-Min Fair Problem Formulation

In this paper, we aim to design the analog beamformer $\mathbf{f}_{RF}$ that maximizes the minimum received SNR among all users. The MMF problem is formulated as

$$\begin{aligned} &\max_{\mathbf{f}_{RF}} \ \min_k \left\{\frac{\left|\mathbf{h}_k^H \mathbf{f}_{RF}\right|^2}{\sigma_k^2}\right\}_{k=1}^K \\ &\text{s.t.} \ |\mathbf{f}_{RF}(i)| = \sqrt{\frac{P}{N_t}}, \ i = 1, \ldots, N_t. \end{aligned} \tag{5}$$

The optimization problem (5) is obviously a non-convex NP-hard problem. A common approach is based on the SDR method, which relaxes the constant amplitude constraint first and calculates the optimal unconstrained solution, followed by a randomization procedure to obtain a good design of analog beamformer. However, this SDR-based analog beamformer will cause notable performance loss and is not computationally efficient. In the next section, we turn to seek a near-optimal analog beamformer design to reduce the complexity while maintaining a satisfactory performance for the mmWave multicast system.

III. Proposed Low-Complexity Analog Beamformer Design

In this section, we first focus on the analog beamformer design problem (5), which is the case that the PSs have infinite resolution (i.e., continuous phase). Then, we will continue the investigation on the analog beamformer design with finite resolution PSs (i.e., discrete phase).

A. Analog Beamformer Design With Infinite Resolution PSs

According to the original objective function (5), we propose a sub-optimal problem reformulation and iteratively refine the solution of it until convergency is achieved. The main idea of our proposed algorithm is individually determining each element of the analog beamformer while assuming the other elements are fixed to conditionally maximize the minimum SNR. To be specific, we rewrite the objective function (5) as

$$\begin{aligned} &\max_{\mathbf{f}_{RF}(i)} \ \min_k \left\{\frac{\left|\mathbf{h}_k^*(i)\mathbf{f}_{RF}(i) + \chi_{\setminus i}^k\right|^2}{\sigma_k^2}\right\}_{k=1}^K \\ &\text{s.t.} \ |\mathbf{f}_{RF}(i)| = \sqrt{\frac{P}{N_t}}, \end{aligned} \tag{6}$$

where $\chi_{\backslash i}^{k} \triangleq \sum_{j \neq i}^{N_t} \mathbf{h}_k^*(j)\mathbf{f}_{RF}(j)$, $k = 1, \ldots, K$, indicates the beamforming gain excluding the *i*-th antenna element for the *k*-th user. Given a random initialization of the beamformer, the *i*-th element of $\mathbf{f}_{RF}$, $i = 1, \ldots, N_t$ is successively designed based on (6) assuming the term $\chi_{\backslash i}^{k}$ is fixed. Therefore, instead of directly solving problem (5) which is intractable, we successively seek the solution to problem (6) for each element of $\mathbf{f}_{RF}$, and then updated through an iterative procedure until the convergency is achieved.

Now, we aim to find the optimal design of $\mathbf{f}_{RF}(i)$ in (6). Notice that the design of $\mathbf{f}_{RF}(i)$ is equivalent to find the optimal phase of it. Let ϕ_i be the phase of $\mathbf{f}_{RF}(i)$, i.e., $\mathbf{f}_{RF}(i) = \sqrt{\frac{P}{N_t}} e^{j\phi_i}$. For the purpose of clear description, we define *K* SNR functions $g_k(\phi_i)$, $k = 1, \ldots, K$, for each user with respect to the phase ϕ_i:

$$
\begin{aligned}
g_1(\phi_i) &= \frac{\left|\mathbf{h}_1^*(i)\sqrt{\frac{P}{N_t}} e^{j\phi_i} + \chi_{\backslash i}^{1}\right|^2}{\sigma_1^2}, \\
&\vdots \\
g_K(\phi_i) &= \frac{\left|\mathbf{h}_K^*(i)\sqrt{\frac{P}{N_t}} e^{j\phi_i} + \chi_{\backslash i}^{K}\right|^2}{\sigma_K^2},
\end{aligned} \tag{7}
$$

Then, obtaining the optimal value of $\mathbf{f}_{RF}(i)$ in problem (6) is equivalent to finding the optimal phase $\phi_i^\star$, at which the minimum SNR value $\min\{g_k(\phi_i^\star)\}_{k=1}^K$ achieves the largest. Since every SNR function is a periodic function with period 2π, we only need to calculate the optimal phase in any 2π interval, and problem (6) is equivalently reformulated as

$$
\phi_i^\star = \max_{\phi_i \in [-\pi, \pi]} \min_k \{g_k(\phi_i)\}_{k=1}^K. \tag{8}
$$

In the following, we present a simple searching algorithm to find the optimal phase $\phi_i^\star$.

We first calculate the achievable maximum SNR_k of each user, denoted as $g_k(\phi_i^k)$, $k = 1, \ldots, K$, and ϕ_i^k is the optimal phase to maximize corresponding $g_k(\phi_i)$, which is computed by

$$
\phi_i^k = \angle \chi_{\backslash i}^{k} - \angle \sqrt{\frac{P}{N_t}} \mathbf{h}_k^*(i), \ k = 1, \ldots, K. \tag{9}
$$

The user whose maximum SNR is the smallest is picked up:

$$
\widetilde{k} = \arg\min_k \ g_k\left(\phi_i^k\right). \tag{10}
$$

We can obtain that $\phi_i^{\widetilde{k}}$ is the optimal phase to maximize the SNR of the $\widetilde{k}$-th user $g_{\widetilde{k}}(\phi_i)$. If we apply the phase $\phi_i^{\widetilde{k}}$ to all users, we can obtain the SNRs of all users, denoted as $g_k(\phi_i^{\widetilde{k}})$, $k = 1, \ldots, K$. Then, there are two possibilities: $g_{\widetilde{k}}(\phi_i^{\widetilde{k}})$ is the minimum among $g_k(\phi_i^{\widetilde{k}})$, $k = 1, \ldots, K$, or not. When $g_{\widetilde{k}}(\phi_i^{\widetilde{k}})$ is the minimum, i.e., the $\widetilde{k}$-th user has achieved its largest SNR $g_{\widetilde{k}}(\phi_i^{\widetilde{k}})$, but this value is still the lowest among all users when $\phi_i = \phi_i^{\widetilde{k}}$, we have the following proposition, whose proof is provided in Appendix A.

Proposition 1: If $g_{\widetilde{k}}(\phi_i^{\widetilde{k}})$ is the smallest among $g_k(\phi_i^{\widetilde{k}})$, $k = 1, \ldots, K$, then, $\phi_i^{\widetilde{k}}$ is the optimal phase of the *i*-th antenna element, i.e., $\phi_i^\star = \phi_i^{\widetilde{k}}$, $\mathbf{f}_{RF}^\star(i) = \sqrt{\frac{P}{N_t}} e^{j\phi_i^\star}$. ■

In order to intuitively illustrate the calculation of the optimal phase, we plot the SNR functions of three users versus phase ϕ_i with $\phi_i \in [-\pi, \pi]$, as shown in Fig. 2(a). The optimal phases ϕ_i^1, ϕ_i^2, ϕ_i^3 corresponding to three users are found. We can see that the third user has the minimum largest SNR. Since $g_3(\phi_i^3)$ is still the smallest among $g_1(\phi_i^3)$, $g_2(\phi_i^3)$, and $g_3(\phi_i^3)$, ϕ_i^3 is the optimal phase and $\phi_i^\star = \phi_i^3$.

Proposition 1 indicates that, if we find $\phi_i^{\widetilde{k}}$ and coincidentally $g_{\widetilde{k}}(\phi_i^{\widetilde{k}})$ is the minimum value among $g_k(\phi_i^{\widetilde{k}})$, $k = 1, \ldots, K$, we can obtain the optimal solution of (6) and the optimal phase searching procedure completes. Otherwise, the optimal phase searching procedure continues based on a necessary condition of the optimal $\phi_i^\star$ presented in the following proposition, whose proof is offered in Appendix B.

Proposition 2: If $g_{\widetilde{k}}(\phi_i^{\widetilde{k}})$ is not the minimum SNR among $g_k(\phi_i^{\widetilde{k}})$, $k = 1, \ldots, K$, the optimal phase $\phi_i^\star$ must be an intersection point of two SNR functions, i.e., at least two users exhibit the same SNR value when $\mathbf{f}_{RF}^\star(i) = \sqrt{\frac{P}{N_t}} e^{j\phi_i^\star}$. ■

According to Proposition 2, we only need to find all the intersection points of SNR functions, and search over these points to obtain the optimal phase. Because the SNR functions have period 2π, we can easily find each intersection point by a bisection based searching procedure. The detailed algorithm for calculating the intersection points of two SNR functions, $g_{k_1}(\phi_i)$ and $g_{k_2}(\phi_i)$ for example, is described in Steps 1-3.

Step 1: Let $\Delta\phi_i^{(t)}$ denote the length of searching interval at the *t*-th iteration, and the searching length is initialized as 2π, i.e., $\Delta\phi_i^{(0)} = 2\pi$. Set ε as the minimum length of searching interval of an intersection point and ν as the searching accuracy of an intersection.

Step 2: If $\Delta\phi_i^{(t)} \geq \varepsilon$, we reduce the length of searching interval by half, i.e., $\Delta\phi_i^{(t+1)} = \frac{\Delta\phi_i^{(t)}}{2}$, and formulate $\frac{2\pi}{\Delta\phi_i^{(t+1)}}$ sub-intervals as $[0, \Delta\phi_i^{(t+1)}], [\Delta\phi_i^{(t+1)}, 2\Delta\phi_i^{(t+1)}], \ldots, [(\frac{2\pi}{\Delta\phi_i^{(t+1)}} - 1)\Delta\phi_i^{(t+1)}, 2\pi]$. If $\Delta\phi_i^{(t+1)} < \varepsilon$, the searching procedure stops.

Step 3: Plug the borders of each sub-interval into $[g_{k_1}(\phi_i^l) - g_{k_2}(\phi_i^l)][g_{k_1}(\phi_i^u) - g_{k_2}(\phi_i^u)]$, in which ϕ_i^l is substituted by each lower border and ϕ_i^u is substituted by each upper border. If the m-th interval satisfies $[g_{k_1}((m-1)\Delta\phi_i^{(t+1)}) - g_{k_2}((m-1)\Delta\phi_i^{(t+1)})][g_{k_1}(m\Delta\phi_i^{(t+1)}) - g_{k_2}(m\Delta\phi_i^{(t+1)})] < 0$, which means there should be one intersection point in the range of $[(m-1)\Delta\phi_i^{(t+1)}, m\Delta\phi_i^{(t+1)}]$, we calculate the intersection phase point based on bisection method with accuracy ν. Otherwise, go back to *Step* 2.

Let set $\mathcal{S}$ store all the intersections. Finally, we can find the optimal phase $\phi_i^\star$ by searching over $\mathcal{S}$, and the problem is presented as

$$
\phi_i^\star = \max_{\phi_i \in \mathcal{S}} \min_k \{g_k(\phi_i)\}_{k=1}^K. \tag{11}
$$

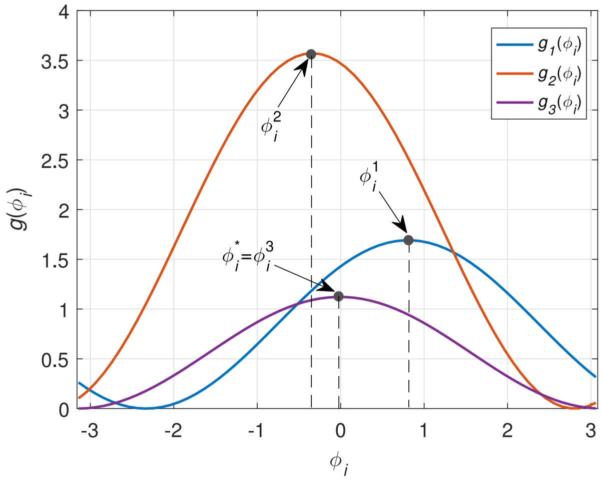

(a)

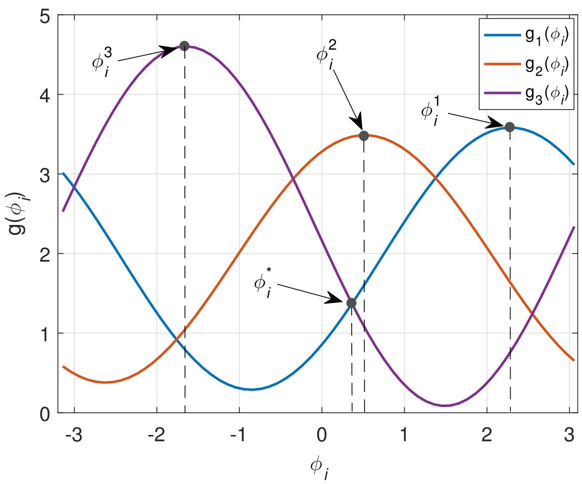

(b)

Fig. 2. Two conditions of the optimal phase $\phi_i^\star$. (a) The optimal phase $\phi_i^\star$ is obtained based on Proposition 1. (b) The optimal phase $\phi_i^\star$ is obtained based on Proposition 2.

We also plot the curves of $g_k(\phi_i), k = 1, 2, 3$ in Fig. 2(b) to help better understand the feasibility of Proposition 2. First, the corresponding optimal phases ϕ_i^1, ϕ_i^2, ϕ_i^3 for each user are calculated. It can be observed that user-2 exhibits the minimum largest SNR. However, at phase ϕ_i^2, $g_1(\phi_i^2)$ and $g_3(\phi_i^2)$ are smaller than $g_2(\phi_i^2)$ and $g_2(\phi_i^2)$ is not the smallest. Under this situation, the optimal phase $\phi_i^\star$ is the intersection point which results in the largest minimum SNR, as shown in the figure.

Thus far, the optimal element of $\mathbf{f}_{RF}$ can be successively determined by the above optimal phase searching algorithm. Note that each element of $\mathbf{f}_{RF}$ is updated by finding the best solution to conditionally optimize (6), if we cannot find a better solution than the current one, we can at least leave it unchanged and the objective remains the same, i.e., *it does not decrease*. Therefore, the proposed iterative procedure is monotonically non-decreasing and can converge to at least a local optimum. Besides, we also simulate the performance

---

Algorithm 1 Analog Beamformer Design With Infinite Resolution PSs

Input: $\mathbf{h}_k$, $k = 1, \ldots, K$, $\mathbf{f}_{RF} = \mathbf{0}$.

1: **while** no convergence **do**
2:   **for** $i = 1 : N_t$ **do**
3:     Calculate optimal phase ϕ_i^k, $k = 1, \ldots, K$, of each user as in (9).
4:     Find the user $\widetilde{k}$ whose maximum SNR is the smallest as in (10).
5:     Calculate SNR values $g_1(\phi_i^{\widetilde{k}}), \ldots, g_K(\phi_i^{\widetilde{k}})$ of all users at the phase point $\phi_i^{\widetilde{k}}$.
6:     **if** $g_{\widetilde{k}}(\phi_i^{\widetilde{k}})$ is the smallest among $\{g_k(\phi_i^{\widetilde{k}})\}_{k=1}^K$ **then**
7:       $\phi_i^\star = \phi_i^{\widetilde{k}}$.
8:     **else**
9:       Find all intersection phase points of any two SNR functions based on Steps 1-3, and them in $\mathcal{S}$.
10:       Obtain the optimal phase $\phi_i^\star$ based on (11).
11:     **end if**
12:   **end for**
13: **end while**
14: $\mathbf{f}_{RF}^\star(i) = \sqrt{\frac{P}{N_t}} e^{j\phi_i^\star}$, $i = 1, \ldots, N_t$.
15: **return** $\mathbf{f}_{RF}^\star$.

---

with different initial beamformers and find that the initializations will not affect the performance too much. Therefore, we take all-zeros vector as the initial beamformer. The complete analog beamformer design with infinite resolution PSs is summarized in Algorithm 1. We can observe from Algorithm 1 that the computation times of intersection points of each antenna element is $\frac{K(K-1)}{2}$, which is determined by the number of users. The computational complexity of the proposed algorithm is $\mathcal{O}(N_{iter}K^2N_t)$, where N_{iter} is the total number of iterations. The complexities of the proposed analog beamformer designs are linear in the number of transmit antennas, which are lower than SDR-based analog beamforming with polynomial complexity.

B. Analog Beamformer Design With Finite Resolution PSs

In order to further reduce the hardware complexity and power consumption, next we consider the analog beamformer design with finite resolution PSs. In this case, each element of $\mathbf{f}_{RF}$ is chosen from a finite set, i.e., $\mathbf{f}_{RF}(i) \in \mathcal{F} \triangleq \{\sqrt{\frac{P}{N_t}} e^{j\frac{2\pi b}{2^B}} \mid b = 1, \ldots, 2^B\}$, $i = 1, \ldots, N_t$, $\mathcal{F}$ is the set of all possible values of each element of analog beamformer and B is the number of bits to control the phase. The discrete phase analog beamformer design can be formulated as

$$\max_{\mathbf{f}_{RF}} \min_{k} \left\{ \frac{\left|\mathbf{h}_k^H \mathbf{f}_{RF}\right|^2}{\sigma_k^2} \right\}_{k=1}^{K} \quad \text{s.t.} \ \mathbf{f}_{RF}(i) \in \mathcal{F}, \ i = 1, \ldots, N_t. \tag{12}$$

The optimal solution can be found by exhaustive search, which has exponential complexity in the number of antennas and is not computationally efficient. Therefore, we propose a low-complexity design of the discrete phase analog beamformer based on an iterative algorithm.

Following the methodology of the individual design on each element in Section III-A, we rewrite the objective (12) as

$$\frac{\left|\mathbf{h}_k^H \mathbf{f}_{RF}\right|^2}{\sigma_k^2} = \frac{\left|\mathbf{h}_k^*(i)\mathbf{f}_{RF}(i) + \chi_{\setminus i}^k\right|^2}{\sigma_k^2},\ k = 1, \ldots, K. \quad (13)$$

Then, the *i*-th element of the analog beamformer $\mathbf{f}_{RF}(i)$ is selected from the set $\mathcal{F}$ assuming the other elements are known to conditionally maximize the minimum SNR among all users:

$$\max_{\mathbf{f}_{RF}(i)} \min_{k} \left\{ \frac{\left|\mathbf{h}_k^*(i)\mathbf{f}_{RF}(i)+\chi_{\setminus i}^k\right|^2}{\sigma_k^2} \right\}_{k=1}^{K}$$
$$\text{s.t. } \mathbf{f}_{RF}(i) \in \mathcal{F}. \quad (14)$$

The complexity of solving this problem is $\mathcal{O}(K|\mathcal{F}|)$. Implementing this procedure from $i = 1$ to $i = N_t$ completes one iteration. Similar to the design of continuous analog beamformer, the convergence of the discrete analog beamformer design is also guaranteed. We repeat it until the convergence is found. The complexity of this iterative algorithm is $\mathcal{O}(K|\mathcal{F}|N_t N_{iter})$, in which N_{iter} is the number of iterations to achieve convergence.

IV. Asymptotically Optimal Analog Beamformer Design and Performance Analysis

Large-scale antenna arrays are usually applied in mmWave systems to provide sufficient beamforming gain. In this case, general beamformer designs, such as the algorithms proposed in the previous section may be not efficient since the complexities increase with the number of transmit antennas. Therefore, more efficient beamformer designs are desired in large-scale mmWave multicast systems. In this section, we investigate the asymptotically optimal analog beamformer designs for the mmWave multicast systems assuming the number of transmit antennas tends to infinity. Benefiting from the asymptotic characteristic of mmWave channels, we can fast obtain the asymptotically optimal design for unconstrained full-digital beamformer with a closed form, which provides the foundation for analog beamformer design, and its asymptotic performance is analyzed as the benchmark. Then, a simple analog beamformer design is proposed, and the performance lower-bound is also provided for evaluating the achievable SNR in large-scale mmWave multicast analog beamforming systems.

A. Asymptotically Optimal Full-Digital Beamforming

For large-scale mmWave multicast systems, the asymptotically optimal full-digital beamformer can be efficiently obtained based on the asymptotic characteristic of mmWave channels. The mmWave channel vectors from the BS to each user are modeled as beam steerings, which are asymptotically orthogonal to each other [35], i.e., when $N_t \to \infty$, the beam steerings $\mathbf{a}_t(\theta_k) \perp \mathbf{a}_t(\theta_l)$ for $\theta_k \neq \theta_l$. Therefore, under the mmWave communication circumstance whose channels have strong directionality and are asymptotically orthogonal, the optimal beamformer is equivalent to generating *K* orthogonal narrow beams with different powers to fairly serve the *K* users. Inspired by [36], we have the following proposition which provides the structure of asymptotically optimal full-digital beamformer for mmWave multicast systems. The proof of it is presented in Appendix C.

Proposition 3: When the number of antennas N_t tends to infinity, the asymptotically optimal full-digital beamformer $\mathbf{f}_{FD}$ has the form of a linear combination of beam steering vectors between the BS and different users:

$$\mathbf{f}_{FD} = \frac{\sum_{k=1}^{K} \xi_k \mathbf{a}_t(\theta_k)}{\beta}, \quad (15)$$

where $\xi_k \in \mathbb{R}$, $k = 1, \ldots, K$, are the weight coefficients for different beam steering vectors, β is the normalization factor. ■

Next, we attempt to find the optimal ξ_k, $k = 1, \ldots, K$, and β in order to construct the optimal beamformer as in (15). Obviously, the normalization factor β can be calculated as

$$\beta = \frac{\left\|\sum_{k=1}^{K} \xi_k \mathbf{a}_t(\theta_k)\right\|}{\sqrt{P}}, \quad (16)$$

and the asymptotic behave of β^2 is derived as

$$\begin{aligned}\lim_{N_t\to\infty} \beta^2 &= \lim_{N_t\to\infty} \frac{1}{P}\left(\sum_{k=1}^{K} \xi_k \mathbf{a}_t(\theta_k)\right)^H \sum_{k=1}^{K} \xi_k \mathbf{a}_t(\theta_k) \\ &= \lim_{N_t\to\infty} \frac{1}{P}\sum_{k=1}^{K}\sum_{l=1}^{K} \xi_k \xi_l \mathbf{a}_t^H(\theta_k)\mathbf{a}_t(\theta_l) \\ &= \frac{1}{P}\sum_{k=1}^{K} \xi_k^2. \end{aligned} \quad (17)$$

Then, the asymptotic SNR_k of the *k*-th user is calculated as

$$\begin{aligned}\lim_{N_t\to\infty} \mathrm{SNR}_k &= \lim_{N_t\to\infty} \frac{\left|\mathbf{h}_k^H \mathbf{f}_{FD}\right|^2}{\sigma_k^2} \\ &= \lim_{N_t\to\infty} \frac{\frac{PN_t|\alpha_k|^2}{\sum_{l=1}^{K}\xi_l^2}\left|\mathbf{a}_t^H(\theta_k)\sum_{l=1}^{K}\xi_l \mathbf{a}_t(\theta_l)\right|^2}{\sigma_k^2} \\ &= \frac{E|\alpha_k|^2\xi_k^2}{\sigma_k^2\sum_{l=1}^{K}\xi_l^2}, \end{aligned} \quad (18)$$

in which we define $E \triangleq PN_t$ to indicate a specific value for an asymptotic system. We assume E is fixed and the power *P* is scaled with the number of transmit antennas N_t [36]. Note that only the ratio among ξ_k^2, $k = 1, \ldots, K$, determines the structure of the full-digital beamformer $\mathbf{f}_{FD}$ and the achievable SNR. The summation $\sum_{k=1}^{K}\xi_k^2$ will not effect the structure of the obtained beamformer since the beamformer will be scaled by the normalization factor β. Therefore, we assume $\sum_{k=1}^{K}\xi_k^2 = 1$, and the optimization of ξ_k, $k = 1, \ldots, K$, can be formulated as

$$\max_{\xi_k} \min_{k} \left\{\frac{E|\alpha_k|^2\xi_k^2}{\sigma_k^2}\right\}_{k=1}^{K}$$
$$\text{s.t. } \sum_{k=1}^{K}\xi_k^2 = 1. \quad (19)$$

The optimal value of ξ_k, $k = 1, \ldots, K$, are obtained to make the SNRs of all users equal [36], which is given by

$$\xi_k = \sqrt{\frac{1}{\sum_{l=1}^{K} \frac{|\alpha_k|^2 \sigma_l^2}{|\alpha_l|^2 \sigma_k^2}}}, \ k = 1, \ldots, K. \tag{20}$$

Hence, the asymptotically optimal full-digital beamformer with the optimal ξ_k, $k = 1, \ldots, K$, is represented as

$$\mathbf{f}_{FD} = \sum_{k=1}^{K} \frac{\mathbf{a}_t(\theta_k)}{\sqrt{\sum_{l=1}^{K} \frac{|\alpha_k|^2 \sigma_l^2}{|\alpha_l|^2 \sigma_k^2}}}. \tag{21}$$

Then, using the full-digital beamformer in (21), the asymptotically SNR_k^{FD} achieved by each user is

$$\lim_{N_t \to \infty} \mathrm{SNR}_k^{FD} = \frac{E|\alpha_k|^2}{\sigma_k^2 \sum_{l=1}^{K} \frac{|\alpha_k|^2 \sigma_l^2}{|\alpha_l|^2 \sigma_k^2}}, \ k = 1, \ldots, K. \tag{22}$$

B. Asymptotically Optimal Analog Beamforming

Based on the findings of the asymptotically optimal full-digital beamformer design in the previous section, we then propose a simple asymptotically optimal analog beamformer design for both infinite and finite resolution PSs. The asymptotic performance lower bounds of the proposed designs are also derived, which can be used to evaluate the achievable SNR of large-scale analog beamformers in mmWave multicast systems.

When infinite resolution PSs are applied, we propose to directly normalize the magnitude of each element of optimal full-digital beamformer $\mathbf{f}_{FD}$ to obtain the analog beamformer for large-scale beamforming systems, i.e.,

$$\mathbf{f}_{RF}(i) = \sqrt{\frac{P}{N_t}} e^{j \angle \mathbf{f}_{FD}(i)}, \ i = 1, \ldots, N_t. \tag{23}$$

The lower bound of the achievable SNR using this design is presented in the following lemma, whose proof is shown in Appendix D.

Lemma 1: When the analog beamformer shown in (23) is applied, the asymptotically achievable SNR_k^{I-PS} of each user is bounded as

$$\lim_{N_t \to \infty} \mathrm{SNR}_k^{I-PS} \geq \frac{E|\alpha_k|^2 \xi_k^2}{\sigma_k^2 \left| \sum_{l=1}^{K} \xi_l \right|^2}, \ k = 1, \ldots, K, \tag{24}$$

in which ξ_k, $k = 1, \ldots, K$, are given by (20). ∎

For the case of finite resolution PSs, we propose to design the analog beamformer by directly quantizing each element of $\mathbf{f}_{FD}$ to the finite set:

$$\begin{aligned} \min_{\mathbf{f}_{RF}(i)} \ & |\mathbf{f}_{RF}(i) - \mathbf{f}_{FD}(i)| \\ \text{s.t.} \ & \mathbf{f}_{RF}(i) \in \mathcal{F}, \ i = 1, \ldots, N_t. \end{aligned} \tag{25}$$

The performance lower bound of each user using this design is presented in the following lemma, whose proof is offered in Appendix E.

Lemma 2: When B-bit resolution PSs are employed to implement the analog beamformer, the asymptotically achievable SNR_k^{F-PS} of each user is bounded as

$$\begin{aligned} \lim_{N_t \to \infty} \mathrm{SNR}_k^{F-PS} \geq \ & \frac{E|\alpha_k|^2 \xi_k^2}{\sigma_k^2 \left| \sum_{l=1}^{K} \xi_l \right|^2} \cos^2\left(\frac{2\pi}{2^{B+1}}\right), \\ & k = 1, \ldots, K, \end{aligned} \tag{26}$$

where ξ_k, $k = 1, \ldots, K$, are given by (20). ∎

V. Simulation Studies

In this section, we provide the simulation results to illustrate the performance of the proposed efficient analog beamformer designs in mmWave multicast systems. We consider a mmWave multicast system with a BS to simultaneously serve $K = 3$ users [13]. The channel gain is set as $\alpha_k \sim \mathcal{CN}(0, 1)$. We assume the communication from the BS to different users is corrupted by the same noise power, and the variance of Gaussian noise is set as $\sigma_k^2 = 1$, $k = 1, \ldots, K$, for simplicity [13]. In the following, the simulation results of the iteratively analog beamformers proposed in Section III are first presented, then, the asymptotic performance analysis for large-scale mmWave multicast systems is provided.

A. Simulation Results of the Proposed Analog Beamforming

We assume the BS is equipped with a 64-antenna ULA, and the antenna spacing at the BS is $d = \frac{\lambda}{2}$. Fig. 3 shows the minimum SNR among all users as a function of the transmit power. We present performance results of our proposed analog beamformer designs based on infinite resolution PSs (i.e., $B = \infty$) and finite resolution PSs (i.e., $B = 2$, $B = 3$), respectively. The SDR-based full-digital (SDR-FD) beamforming scheme is plotted as the performance benchmark [16]. Besides, for comparison purpose, we also generate SDR-based analog beamformers with continuous phase (FD-C), and with quantized phase (FD-Q) of resolutions $B = 2$, $B = 3$, respectively. We can observe that our proposed algorithms can achieve satisfactory performances and have significant SNR improvement compared to their competitors. Our proposed analog beamforming with two-bit resolution PSs can even outperform the SDR-based analog beamforming with continuous phase (FD-C). Moreover, we can find that even the users are applied with single antenna, the BS can still provide sufficient beamforming gain which combats mmWave channel loss and offers satisfactory quality of service to each user. In Fig. 4, we repeat the same simulation with a 128-ULA and similar conclusions can be drawn. For our considered systems with common settings, the number of iterations N_{iter} is generally between 2 and 5, which demonstrates the quick convergence of the proposed algorithms.

The simulation result of minimum SNR as a function of the number of users K is provided in Fig. 5. We can find that our proposed analog beamforming designs still outperform their competitors, and have notable performance advantages. Besides, it can be seen from Fig. 5 that the minimum SNR would decrease with increasing K, and our proposed approaches decline slower than the SDR-based analog beamformer, which means the proposed approaches are more robust

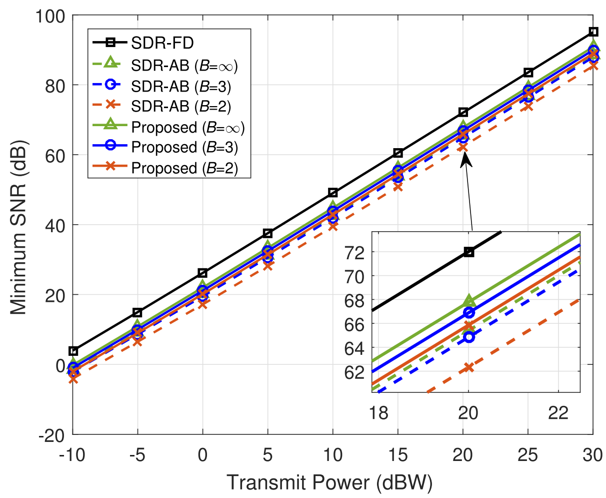

Fig. 3. Minimum SNR versus transmit power P ($N_t = 64$, $K = 3$).

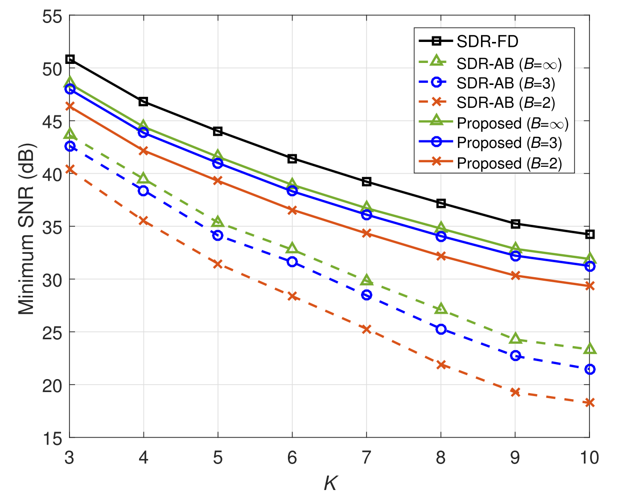

Fig. 5. Minimum SNR versus the number of users K ($P = 10$ dBW, $N_t = 128$).

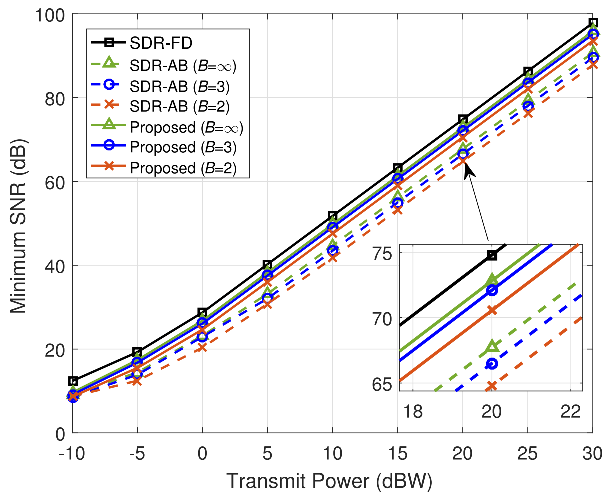

Fig. 4. Minimum SNR versus transmit power P ($N_t = 128$, $K = 3$).

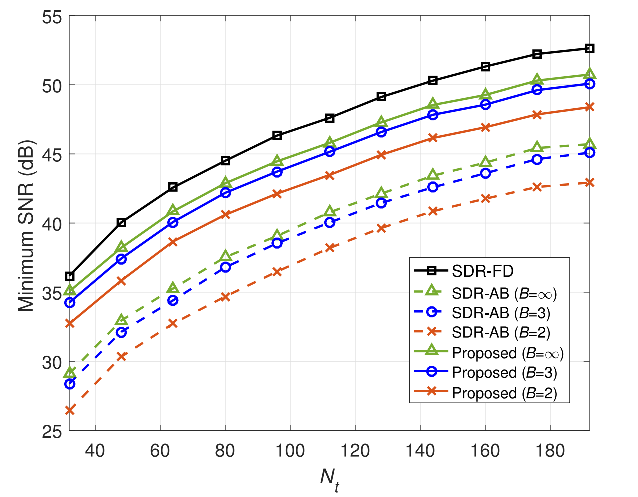

Fig. 6. Minimum SNR versus the number of transmit antennas N_t ($P = 10$ dBW, $K = 3$).

to serving more users. In Fig. 6, we illustrate the minimum SNR versus the number of transmit antennas N_t. It can be seen that the minimum SNR among users improves stably with the increasing number of antennas and the proposed algorithms can always maintain their favorable performance advantages with different number of transmit antennas.

In Fig. 7, we turn to investigate the energy efficiency of mmWave multicast system. In conventional point-to-point or multiuser downlink systems, the energy efficiency is given by the ratio of achievable performance (i.e., spectral efficiency or sum-rate) over the power consumption [14], [17]. However, for multicast transmission, max-min fair is the design criteria and the minimum SNR is a typical metric to evaluate the system performance. By the same token, for our considered MMF based multicast system, we define the energy efficiency by the ratio of minimum spectral efficiency over the transmit power. The power consumption of an RF chain is set as $P_{RF} = 300$mW [27]. The power consumptions of a PS with different resolutions are set as $P_{PS_C} = 75$mW for continuous phase control, $P_{PS_3} = 60$mW for a three-bit resolution PS, $P_{PS_2} = 40$mW for a two-bit resolution PS [27]. Finally, the transmit power is fixed at $P = 10$dBW. From Fig. 7, we can observe that full-digital beamforming will have dramatic energy efficiency degradation because the large number of RF chains cause huge energy consumption. On the other hand, we can see that PSs based analog beamforming enjoys significant advantages in terms of energy efficiency, which is a preferable choice for energy efficient mmWave multicast communication systems.

In order to evaluate the performance of mmWave multicast systems from a probabilistic perspective, we demonstrate the cumulative distribution function (CDF) of the spectral efficiency in Fig. 8. It can be observed from the simulation curves that the most likely achievable spectral efficiency of each user is between 6 and 7 bit/s/Hz when a 128-ULA analog beamformer is applied, and thus the transmission rate will be significantly improved by exploiting mmWave communications.

B. Asymptotic Performance of Large-Scale mmWave Multicast Systems

Next, we will demonstrate the asymptotic performance of mmWave multicast communications with large-scale antenna

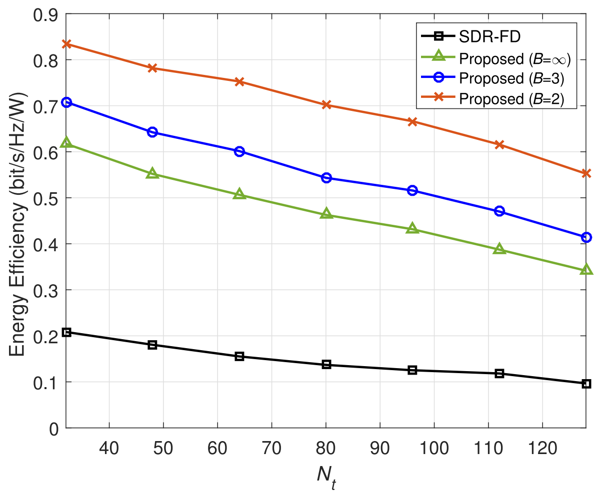

Fig. 7. Energy efficiency versus the number of transmit antennas N_t ($P = 10$ dBW, $K = 3$).

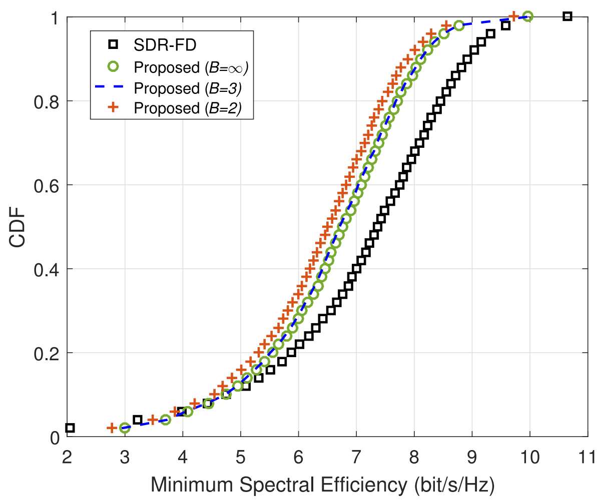

Fig. 8. CDF of the spectral efficiency ($P = 10$ dBW, $N_t = 128$, $K = 3$).

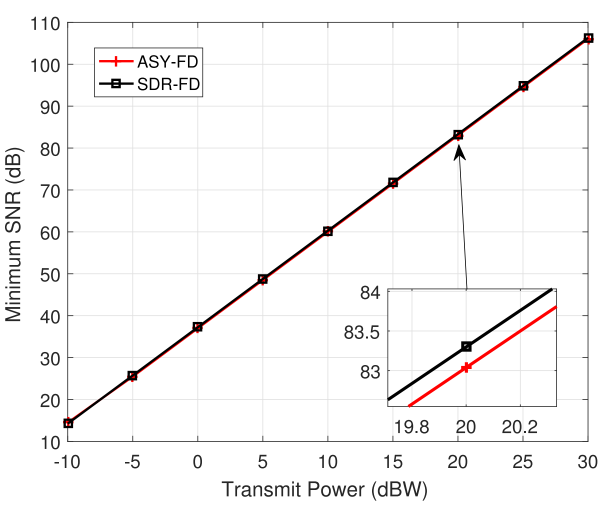

Fig. 9. Minimum SNR versus the transmit power P ($N_t = 256$, $K = 3$).

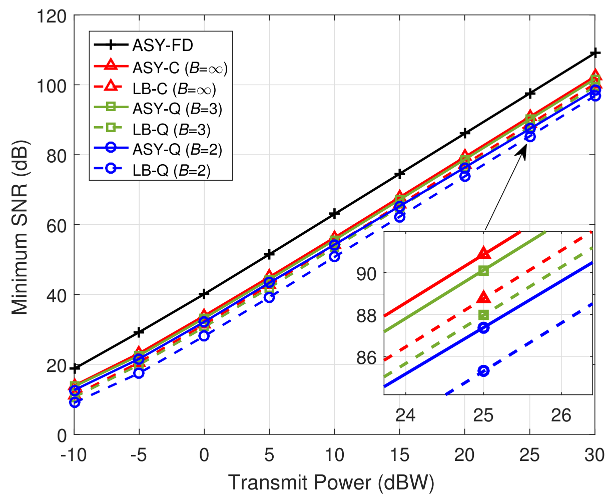

Fig. 10. Performance of asymptotically optimal beamformers with varying transmit power P ($N_t = 512$, $K = 3$).

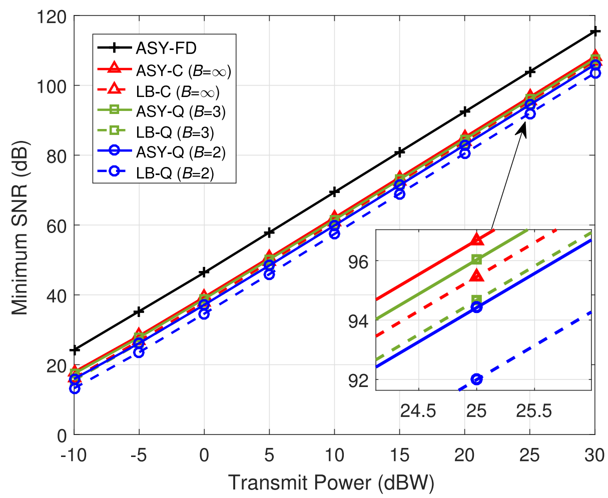

Fig. 11. Performance of asymptotically optimal beamformers with varying transmit power P ($N_t = 1024$, $K = 3$).

arrays. We should note here that mmWave communications can enable larger number of antennas to be packed into a small dimension, the number of transmit antennas considered in a normal scale mmWave systems is usually between 64 and 256 [25]. Therefore, we may roughly set 256 as a boundary for small-scale and large-scale scenarios in this paper. In order to illustrate the validity of the asymptotically optimal beamformer, we show the MMF performance versus the transmit power in Fig. 9, and the number of antennas is set as 256. We can observe from Fig. 9 that the gap between the SDR based full-digital beamformer (SDR-FD) and the asymptotically optimal case (ASY-FD) is really small, which validates the optimality of the proposed schemes in Section IV.

Figs. 10 and 11 present the minimum SNR performance of the proposed asymptotically optimal schemes introduced in Section IV. The performance curves of the asymptotically optimal full-digital beamformer (ASY-FD), the proposed asymptotically optimal analog beamformers with continuous phase (ASY-C) and its lower bound (LB-C), as well as quantized phase (ASY-Q) and its lower bound (LB-Q) are respectively plotted. It can be observed that the performance loss of the asymptotically optimal analog beamformer with infinite resolution PSs comparing with the full-digital case is

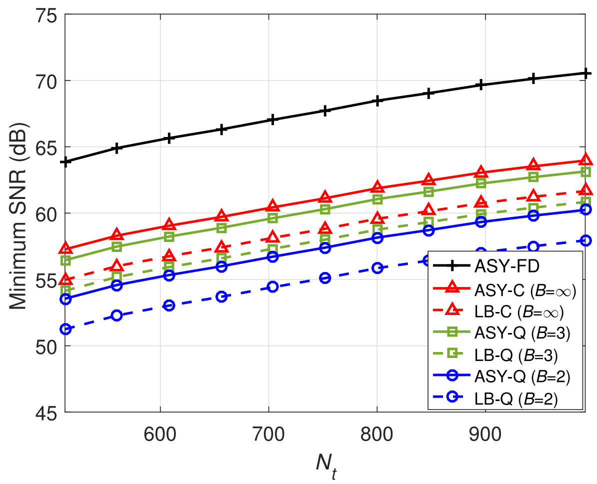

Fig. 12. Performance of asymptotically optimal beamformers with varying number of antennas N_t ($P = 10$ dBW, $K = 3$).

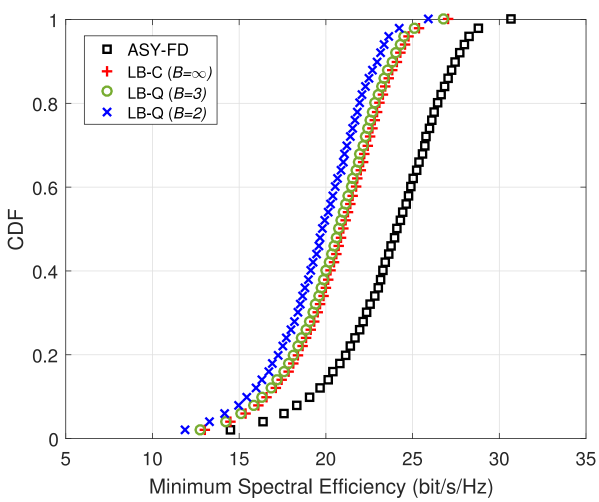

Fig. 13. CDF of the asymptotic spectral efficiency ($P = 10$ dBW, $N_t = 1024$, $K = 3$).

generally no more than 6dB. In view of the hardware efficiency of analog beamforming, this gap is acceptable for mmWave multicast systems.

In Fig. 12, we show the minimum SNR versus the number of transmit antennas N_t. We can observe that the minimum SNR improves steadily with increasing number and the growth rate is relatively slow in very large-scale antenna array systems. Fig. 13 presents the CDF of the asymptotically optimal spectral efficiency as well as the performance lower bounds of analog beamformers. It is shown that when the transmit power is $P = 10$dBW, in more than 50% cases the asymptotically optimal analog beamformer can achieve at least 20 bit/s/Hz spectral efficiency for each user in a 1024-ULA mmWave multicast system. We can conclude that the analog beamforming can potentially achieve transmission rate of several gigabits per second for each user by exploiting the large bandwidth at mmWave bands. Therefore, the proposed efficient analog beamforming is able to simultaneously serve multiple users with satisfactory MMF conditions, and becoming a promising approach for mmWave multicast communications.

VI. Conclusion

This paper investigated the analog beamforming in single-group mmWave multicast systems. We considered the MMF problem and proposed an iterative analog beamformer design. It was shown that our proposed analog beamformer with two-bit resolution PSs can even outperform the SDR-based analog beamforming with continuous phase, and the performance gap between our proposed continuous phase based analog beamformer and the full-digital case is no more than 4dB for a 3-user system. Furthermore, we also studied the asymptotically optimal beamformer design for single-group mmWave multicast systems and derived the asymptotic performance lower-bounds of the proposed analog beamformers. Simulation results demonstrated that for a 3-user multicast system, the performance loss of the asymptotically optimal analog beamformer would be no more than 6dB, which is acceptable for mmWave multicast systems.

Appendix A
Proof of Proposition 1

Assume that $\phi_i^\star$ is the optimal phase of the i-th element of beamformer in (6) and $g_k(\phi_i^\star)$, $k = 1, \ldots, K$, are the resulting SNRs of all users. Let $\gamma_i^\star$ indicate the largest minimum SNR in (6) which is given by the smallest value of $g_k(\phi_i^\star)$ for $k = 1, \ldots, K$, i.e., $\gamma_i^\star = \min\{g_k(\phi_i^\star)\}_{k=1}^K$. If $\phi_i^\star \neq \phi_i^{\widetilde{k}}$, we have $\gamma_i^\star \neq g_{\widetilde{k}}(\phi_i^{\widetilde{k}})$ and $\gamma_i^\star > g_{\widetilde{k}}(\phi_i^{\widetilde{k}})$. Moreover, since $\gamma_i^\star$ is the minimum SNR at point $\phi_i^\star$, we have $\gamma_i^\star \leq g_{\widetilde{k}}(\phi_i^\star)$, then $g_{\widetilde{k}}(\phi_i^{\widetilde{k}}) < \gamma_i^\star \leq g_{\widetilde{k}}(\phi_i^\star)$, which contradicts the fact that $g_{\widetilde{k}}(\phi_i^{\widetilde{k}})$ should be larger than $g_{\widetilde{k}}(\phi_i^\star)$ since $\phi_i^{\widetilde{k}}$ is the optimal condition to the $\widetilde{k}$-user. Therefore, Proposition 1 is proved. ■

Appendix B
Proof of Proposition 2

Given the optimal phase $\phi_i^\star$ of the i-th element of analog beamformer, the SNR values of all users at this point are $g_k(\phi_i^\star)$, $k = 1, \ldots, K$. If Proposition 2 is not true, then the SNRs of all users are different with each other. Without loss of generality, we assume $\gamma_i^\star = g_1(\phi_i^\star) < g_2(\phi_i^\star) < \ldots < g_K(\phi_i^\star)$, and the optimal minimum SNR $\gamma_i^\star$ is equal to $g_1(\phi_i^\star)$ under this situation. Note that each SNR function $g_k(\phi_i)$, $k = 1, \ldots, K$, with period 2π has alternate wave peaks and wave troughs, and $g_1(\phi_i)$ does not achieve its wave peak at $\phi_i^\star$ (otherwise is the condition discussed in Proposition 1). If we adjust $\phi_i^\star$ continuously to the improving direction of function $g_1(\phi_i)$ until its SNR value just exceeds any SNR of the other $K-1$ users at one phase point, then they may achieve the same SNR and the SNR functions of these users may intersect with each other at this point. The new minimum SNR is given by this intersection and is improved compared to $\gamma_i^\star$, which contradicts the assumption that $\gamma_i^\star = g_1(\phi_i^\star)$ is the optimal minimum SNR. Therefore, Proposition 2 must hold for the optimal phase $\phi_i^\star$. ■

Appendix C
Proof of Proposition 3

If we use the asymptotically optimal full-digital beamformer shown in (15), the received signal at the k-th user has the form of

$$\begin{aligned} y_k &= \mathbf{h}_k^H \mathbf{f}_{FD} s + n_k \\ &= \sqrt{P}\sqrt{N_t}\alpha_k \mathbf{a}_t(\theta_k)\frac{\sum_{l=1}^K \xi_l \mathbf{a}_t(\theta_l)}{\beta} s + n_k \\ &\overset{(a)}{\approx} \frac{\sqrt{PN_t}\alpha_k\xi_k}{\beta} s + n_k \\ &= \frac{\sqrt{E}\alpha_k\xi_k}{\beta} s + n_k, \end{aligned} \tag{27}$$

where (a) is based on the fact that beam steerings with different AoDs are asymptotically orthogonal to each other. $E \triangleq PN_t$ is fixed and the power P is scaled with the number of transmit antennas N_t.

Otherwise, if the beamformer does not have this form, then it can be expressed as

$$\mathbf{f}_{FD} = \frac{\sum_{k=1}^K \xi_k \mathbf{a}_t(\theta_k) + \sum_{m=1}^{N_t-K} \mu_m \mathbf{g}_m}{\beta'}, \tag{28}$$

where $\{\mathbf{g}_m\}_{m=1}^{N_t-K}$ is an orthonormal basis of the space orthogonal to the space spanned by $\{\mathbf{a}_t(\theta_k)\}_{k=1}^K$, β' is the normalization factor. Using this beamformer, the received signal at the k-th user is

$$\begin{aligned} y_k &= \mathbf{h}_k^H \mathbf{f}_{FD} s + n_k \\ &= \sqrt{P}\sqrt{N_t}\alpha_k \mathbf{a}_t(\theta_k)\frac{\left(\sum_{l=1}^K \xi_k \mathbf{a}_t(\theta_l) + \sum_{m=1}^{N_t-K}\mu_m \mathbf{g}_m\right)}{\beta'} s \\ &\quad + n_k \\ &\approx \frac{\sqrt{PN_t}\alpha_k\xi_k}{\beta'} s + n_k \\ &= \frac{\sqrt{E}\alpha_k\xi_k}{\beta'} s + n_k. \end{aligned} \tag{29}$$

We can observe from the above expression that the signal power of the k-th user is diminished compared to the condition in (27). The reason is that the new normalization factor β' should satisfy $\beta' > \beta$ to keep the same norm because there is an additional term in the numerator in (28). The additional term $\sum_{m=1}^{N_t-K} \mathbf{g}_m$ will consume the transmit power, but would not contribute to improving the strength of the desired signal. Then, the beamformer can be reconstructed to obtain the optimal beamformer by transforming the power caused by this orthogonal component into generating useful directional beam steerings, and the denominator β' can achieve its smallest value, which is equal to β. Therefore, (15) is proved to be the asymptotically optimal beamformer. ■

Appendix D
Proof of Lemma 1

The analog beamformer in (23) can be rewritten as

$$\mathbf{f}_{RF}(i) = \sqrt{\frac{P}{N_t}} \frac{\sum_{k=1}^K \xi_k e^{j\pi(i-1)\sin\theta_k}}{\left|\sum_{k=1}^K \xi_k e^{j\pi(i-1)\sin\theta_k}\right|},\ i = 1,\ldots,N_t, \tag{30}$$

in which the amplitude of each element is normalized to $\sqrt{\frac{P}{N_t}}$. Then, the asymptotically achievable SNR of the k-th user is written as

$$\begin{aligned} &\lim_{N_t\to\infty} \mathrm{SNR}_k^{I-PS} \\ &= \lim_{N_t\to\infty} \frac{\left|\mathbf{h}_k^H \mathbf{f}_{RF}\right|^2}{\sigma_k^2} \\ &= \lim_{N_t\to\infty} \frac{E|\alpha_k|^2}{\sigma_k^2}\left|\sum_{i=1}^{N_t} \frac{e^{-j\pi(i-1)\sin\theta_k}\sum_{l=1}^K \xi_l e^{j\pi(i-1)\sin\theta_l}}{N_t\left|\sum_{l=1}^K \xi_l e^{j\pi(i-1)\sin\theta_l}\right|}\right|^2 \\ &\overset{(a)}{\geq} \lim_{N_t\to\infty} \frac{E|\alpha_k|^2}{\sigma_k^2}\left|\sum_{i=1}^{N_t} \frac{e^{-j\pi(i-1)\sin\theta_k}\sum_{l=1}^K \xi_l e^{j\pi(i-1)\sin\theta_l}}{N_t\left|\sum_{l=1}^K \xi_l\right|}\right|^2, \end{aligned} \tag{31}$$

in which (a) can be obtained by the following inequation:

$$\left|\sum_{l=1}^K \xi_l e^{j\pi(i-1)\sin\theta_l}\right| \leq \left|\sum_{l=1}^K \xi_l\right|. \tag{32}$$

Then, the last expression in (31) can be rewritten as (33), which is shown at the top of the next page.

It is shown that each term $e^{-j\pi(i-1)\sin\theta_k}\sum_{u\neq k}^K \xi_u e^{j\pi(i-1)\sin\theta_u}$ is a complex number with bounded modulus because θ_k, $k = 1,\ldots,K$, are uniformly distributed in $[-\frac{\pi}{2}, \frac{\pi}{2}]$, and $\theta_k \neq \theta_u$ for $k \neq u$, and the summation $\sum\limits_{u\neq k}^K \xi_u e^{j\pi(i-1)\sin\theta_u}$ is a random complex number with bounded modulus. With $i = 1,\ldots,N_t$, the phases of $e^{-j\pi(i-1)\sin\theta_k}\sum_{u\neq k}^K \xi_u e^{j\pi(i-1)\sin\theta_u}$ are varying from $-\pi$ to π, and the summation of these complex numbers with various phases will also have a bounded amplitude. Hence, when $N_t \to \infty$, the second term of the above equation tends to zero, and the asymptotically achievable SNR_k can be represented as

$$\lim_{N_t\to\infty} \mathrm{SNR}_k^{I-PS} \geq \frac{E|\alpha_k|^2}{\sigma_k^2}\left|\frac{\xi_k}{\sum_{l=1}^K \xi_l}\right|^2 = \frac{E|\alpha_k|^2\xi_k^2}{\sigma_k^2\left|\sum_{l=1}^K \xi_l\right|^2}, \quad k = 1,\ldots,K.$$

Therefore, Lemma 1 is proved. ■

Appendix E
Proof of Lemma 2

Let $\delta_i \triangleq \angle\mathbf{f}_{FD}(i) - \angle\mathbf{f}_{RF}(i)$, $-\frac{2\pi}{2^{B+1}} \leq \delta_i \leq \frac{2\pi}{2^{B+1}}$, indicate the phase quantization error between the i-th element of discrete phase analog beamformer and the optimal unconstrained full-digital beamformer. The asymptotically achievable SNR of the k-th user is represented as

$$\begin{aligned} &\lim_{N_t\to\infty} \mathrm{SNR}_k^{F-PS} \\ &= \lim_{N_t\to\infty} \frac{\left|\mathbf{h}_k^H \mathbf{f}_{RF}\right|^2}{\sigma_k^2} \\ &= \lim_{N_t\to\infty} \frac{E|\alpha_k|^2}{\sigma_k^2}\left|\sum_{i=1}^{N_t} \frac{e^{-j\pi(i-1)\sin\theta_k}\left(\sum_{l=1}^K \xi_l e^{j\pi(i-1)\sin\theta_l}\right)e^{j\delta_i}}{N_t\left|\sum_{l=1}^K \xi_l e^{j\pi(i-1)\sin\theta_l}\right|}\right|^2 \end{aligned}$$

$$\begin{aligned}&\lim_{N_t\to\infty}\frac{E|\alpha_k|^2}{\sigma_k^2}\left|\sum_{i=1}^{N_t}\frac{e^{-j\pi(i-1)\sin\theta_k}\sum_{l=1}^{K}\xi_l e^{j\pi(i-1)\sin\theta_l}}{N_t\left|\sum_{l=1}^{K}\xi_l\right|}\right|^2\\&=\lim_{N_t\to\infty}\frac{E|\alpha_k|^2}{\sigma_k^2}\left|\sum_{i=1}^{N_t}\left(\frac{\xi_k}{N_t\left|\sum_{l=1}^{K}\xi_l\right|}+\frac{e^{-j\pi(i-1)\sin\theta_k}\sum_{u\neq k}^{K}\xi_u e^{j\pi(i-1)\sin\theta_u}}{N_t\left|\sum_{l=1}^{K}\xi_l\right|}\right)\right|^2\\&=\lim_{N_t\to\infty}\frac{E|\alpha_k|^2}{\sigma_k^2}\left|\frac{\xi_k}{\left|\sum_{l=1}^{K}\xi_l\right|}+\frac{\sum_{i=1}^{N_t}\left(e^{-j\pi(i-1)\sin\theta_k}\sum_{u\neq k}^{K}\xi_u e^{j\pi(i-1)\sin\theta_u}\right)}{N_t\left|\sum_{l=1}^{K}\xi_l\right|}\right|^2\end{aligned}\tag{33}$$

$$\begin{aligned}&\lim_{N_t\to\infty}\frac{E|\alpha_k|^2}{\sigma_k^2}\left|\sum_{i=1}^{N_t}\left(\frac{\xi_k(\cos\delta_i+j\sin\delta_i)}{N_t\left|\sum_{l=1}^{K}\xi_l\right|}+\frac{e^{-j\pi(i-1)\sin\theta_k}\left(\sum_{u\neq k}^{K}\xi_u e^{j\pi(i-1)\sin\theta_u}\right)(\cos\delta_i+j\sin\delta_i)}{N_t\left|\sum_{l=1}^{K}\xi_l\right|}\right)\right|^2\\&\overset{(a)}{\geq}\lim_{N_t\to\infty}\frac{E|\alpha_k|^2}{\sigma_k^2}\left|\sum_{i=1}^{N_t}\left(\frac{\xi_k\cos\delta_i}{N_t\left|\sum_{l=1}^{K}\xi_l\right|}+\frac{e^{-j\pi(i-1)\sin\theta_k}\left(\sum_{u\neq k}^{K}\xi_u e^{j\pi(i-1)\sin\theta_u}\right)\cos\delta_i}{N_t\left|\sum_{l=1}^{K}\xi_l\right|}\right)\right|^2\end{aligned}\tag{35}$$

$$\geq\lim_{N_t\to\infty}\frac{E|\alpha_k|^2}{\sigma_k^2}\left|\sum_{i=1}^{N_t}\frac{e^{-j\pi(i-1)\sin\theta_k}\left(\sum_{l=1}^{K}\xi_l e^{j\pi(i-1)\sin\theta_l}\right)e^{j\delta_i}}{N_t\left|\sum_{l=1}^{K}\xi_l\right|}\right|^2\tag{34}$$

Then, similar to the derivation in (33), and given $e^{j\delta_i}=\cos\delta_i+j\sin\delta_i$, (34) can be written as (35), which is presented at the top of this page. (a) is hold based on the fact that $|X+Y|\geq|X|$. Since $-\frac{2\pi}{2^{B+1}}\leq\delta_i\leq\frac{2\pi}{2^{B+1}}$, we have $\cos\delta_i\geq\cos(\frac{2\pi}{2^{B+1}})$. Therefore, we can obtain

$$\begin{aligned}&\lim_{N_t\to\infty}\mathrm{SNR}_k^{F-PS}\\&\geq\lim_{N_t\to\infty}\frac{E|\alpha_k|^2}{\sigma_k^2}\\&\quad\times\left|\sum_{i=1}^{N_t}\left(\frac{\xi_k\cos\left(\frac{2\pi}{2^{B+1}}\right)}{N_t\left|\sum_{l=1}^{K}\xi_l\right|}\right.\right.\\&\qquad\left.\left.+\frac{e^{-j\pi(i-1)\sin\theta_k}(\sum_{u\neq k}^{K}\xi_u e^{j\pi(i-1)\sin\theta_u})\cos\left(\frac{2\pi}{2^{B+1}}\right)}{N_t\left|\sum_{l=1}^{K}\xi_l\right|}\right)\right|^2\\&=\lim_{N_t\to\infty}\frac{E|\alpha_k|^2}{\sigma_k^2}|\frac{\xi_k\cos\left(\frac{2\pi}{2^{B+1}}\right)}{\left|\sum_{l=1}^{K}\xi_l\right|}\\&\quad+\frac{\sum_{i=1}^{N_t}\left(e^{-j\pi(i-1)\sin\theta_k}(\sum_{u\neq k}^{K}\xi_u e^{j\pi(i-1)\sin\theta_u})\cos\left(\frac{2\pi}{2^{B+1}}\right)\right)}{N_t\left|\sum_{l=1}^{K}\xi_l\right|}|^2\\&\overset{(b)}{=}\lim_{N_t\to\infty}\frac{E|\alpha_k|^2}{\sigma_k^2}\left|\frac{\xi_k\cos\left(\frac{2\pi}{2^{B+1}}\right)}{\left|\sum_{l=1}^{K}\xi_l\right|}\right|^2=\frac{E|\alpha_k|^2\xi_k^2}{\sigma_k^2\left|\sum_{l=1}^{K}\xi_l\right|^2}\cos^2\left(\frac{2\pi}{2^{B+1}}\right),\end{aligned}\tag{36}$$

in which (b) can be obtained following the similar method as in Appendix D. ■

REFERENCES

[1] Z. Wang, H. Li, M. Li, and W. Kellerer, "Efficient analog beamforming for max–min fair multicast transmission," in *Proc. IEEE Veh. Technol. Conf. (VTC)*, Kuala Lumpur, Malaysia, Apr. 2019, pp. 1–5.

[2] A. L. Swindlehurst, E. Ayanoglu, P. Heydari, and F. Capolino, "Millimeter-wave massive MIMO: The next wireless revolution?" *IEEE Commun. Mag.*, vol. 52, no. 9, pp. 56–62, Sep. 2014.

[3] A. Alkhateeb, J. Mo, N. González-Prelcic, and R. W. Heath, Jr., "MIMO precoding and combining solutions for millimeter-wave systems," *IEEE Commun. Mag.*, vol. 52, no. 12, pp. 122–131, Dec. 2014.

[4] T. S. Rappaport *et al.*, "Millimeter wave mobile communications for 5G cellular: It will work!" *IEEE Access*, vol. 1, pp. 335–349, 2013.

[5] M. M. Mowla, I. Ahmad, D. Habibi, and Q. V. Phung, "A green communication model for 5G systems," *IEEE Trans. Green Commun. Netw.*, vol. 1, no. 3, pp. 264–280, Sep. 2017.

[6] R. W. Heath, Jr., N. González-Prelcic, S. Rangan, W. Roh, and A. M. Sayeed, "An overview of signal processing techniques for millimeter wave MIMO systems," *IEEE J. Sel. Topics Signal Process.*, vol. 10, no. 3, pp. 436–453, Apr. 2016.

[7] R. Méndez-Rial, C. Rusu, N. González-Prelcic, and A. Alkhateeb, "Hybrid MIMO architectures for millimeter wave communications: Phase shifters or switches?" *IEEE Access*, vol. 4, pp. 247–267, 2016.

[8] P. Raviteja, Y. Hong, and E. Viterbo, "Analog beamforming with low resolution phase shifters," *IEEE Wireless Commun. Lett.*, vol. 6, no. 4, pp. 502–505, Aug. 2017.

[9] Y. Sun and C. Qi, "Weighted sum-rate maximization for analog beamforming and combining in millimeter wave massive MIMO communications," *IEEE Commun. Lett.*, vol. 21, no. 8, pp. 1883–1886, Aug. 2017.

[10] T. S. Rappaport *et al.*, "Overview of millimeter wave communications for fifth-generation (5G) wireless networks—With a focus on propagation models," *IEEE Trans. Antennas Propag.*, vol. 65, no. 12, pp. 6213–6230, Dec. 2017.

[11] W. Roh *et al.*, "Millimeter-wave beamforming as an enabling technology for 5G cellular communications: Theoretical feasibility and prototype results," *IEEE Commun. Mag.*, vol. 52, no. 2, pp. 106–113, Feb. 2014.

[12] S. Han, C.-L. I, Z. Xu, and C. Rowell, "Large-scale antenna systems with hybrid analog and digital beamforming for millimeter wave 5G," *IEEE Commun. Mag.*, vol. 53, no. 1, pp. 186–194, Jan. 2015.

[13] A. Alkhateeb, G. Leus, and R. W. Heath, Jr., "Limited feedback hybrid precoding for multi-user millimeter wave systems," *IEEE Trans. Wireless Commun.*, vol. 14, no. 11, pp. 6481–6494, Nov. 2015.

[14] A. Li and C. Masouros, "Hybrid analog–digital millimeter-wave MU-MIMO transmission with virtual path selection," *IEEE Commun. Lett.*, vol. 21, no. 2, pp. 438–441, Feb. 2017.

[15] Z. Li, S. Han, S. Sangodoyin, R. Wang, and A. F. Molisch, "Joint optimization of hybrid beamforming for multi-user massive MIMO downlink," *IEEE Trans. Wireless Commun.*, vol. 17, no. 6, pp. 3600–3614, Jun. 2018.

[16] N. D. Sidiropoulos, T. N. Davidson, and Z.-Q. Luo, "Transmit beamforming for physical-layer multicasting," *IEEE Trans. Signal Process.*, vol. 54, no. 6, pp. 2239–2251, Jun. 2006.

[17] X. Yu, J.-C. Shen, J. Zhang, and K. B. Letaief, "Alternating minimization algorithms for hybrid precoding in millimeter wave MIMO systems," *IEEE J. Sel. Topics Signal Process.*, vol. 10, no. 3, pp. 485–500, Apr. 2016.

[18] C. Rusu, R. Méndez-Rial, N. González-Prelcic, and R. W. Heath, Jr., "Low complexity hybrid sparse precoding and combining in millimeter wave MIMO systems," in *Proc. IEEE Int. Conf. Commun. (ICC)*, London, U.K., Jun. 2015, pp. 1340–1345.

[19] S. He, C. Qi, Y. Wu, and Y. Huang, "Energy-efficient transceiver design for hybrid sub-array architecture MIMO systems," *IEEE Access*, vol. 4, pp. 9895–9905, 2016.

[20] X. Gao, L. Dai, S. Han, C.-L. I, and R. W. Heath, Jr., "Energy-efficient hybrid analog and digital precoding for mmWave MIMO systems with large antenna arrays," *IEEE J. Sel. Areas Commun.*, vol. 34, no. 4, pp. 998–1009, Apr. 2016.

[21] M. Li, Z. Wang, X. Tian, and Q. Liu, "Joint hybrid precoder an combiner design for multi-stream transmission in mmWave MIMO systems," *IET Commun.*, vol. 11, no. 7, pp. 2596–2604, Nov. 2017.

[22] F. Sohrabi and W. Yu, "Hybrid digital and analog beamforming design for large-scale antenna arrays," *IEEE J. Sel. Topics Signal Process.*, vol. 10, no. 3, pp. 501–513, Apr. 2016.

[23] J.-C. Chen, "Hybrid beamforming with discrete phase shifters for millimeter-wave massive MIMO systems," *IEEE Trans. Veh. Technol.*, vol. 66, no. 8, pp. 7604–7608, Aug. 2017.

[24] Z. Wang, M. Li, Q. Liu, and A. L. Swindlehurst, "Hybrid precoder and combiner design with low resolution phase shifters in mmWave MIMO systems," *IEEE J. Sel. Topics Signal Process.*, vol. 12, no. 2, pp. 1–14, May 2018.

[25] O. E. Ayach, S. Rajagopal, S. Abu-Surra, Z. Pi, and R. W. Heath, Jr., "Spatially sparse precoding in millimeter wave MIMO systems," *IEEE Trans. Wireless Commun.*, vol. 13, no. 3, pp. 1499–1513, Mar. 2014.

[26] J. Zhang, Y. Huang, Q. Shi, J. Wang, and L. Yang, "Codebook design for beam alignment in millimeter wave communication systems," *IEEE Trans. Commun.*, vol. 65, no. 11, pp. 4980–4995, Jul. 2017.

[27] M. Li, Z. Wang, H. Li, Q. Liu, and L. Zhou, "A hardware-efficient hybrid beamforming solution for mmWave MIMO systems," *IEEE Wireless Commun.*, vol. 26, no. 1, pp. 137–143, Feb. 2019.

[28] X. Gao, L. Dai, Y. Sun, S. Han, and C.-L. I, "Machine learning inspired energy-efficient hybrid precoding for mmWave massive MIMO systems," in *Proc. IEEE Int. Conf. Commun. (ICC)*, Paris, France, May 2017, pp. 1–6.

[29] E. Karipidis, N. D. Sidiropoulos, and Z.-Q. Luo, "Quality of service and max–min fair transmit beamforming to multiple cochannel multicast groups," *IEEE Trans. Signal Process.*, vol. 56, no. 3, pp. 1268–1279, Mar. 2008.

[30] M. Sadeghi, L. Sanguinetti, R. Couillet, and C. Yuen, "Reducing the computational complexity of multicasting in large-scale antenna systems," *IEEE Trans. Wireless Commun.*, vol. 16, no. 5, pp. 2963–2975, May 2017.

[31] E. Chen and M. Tao, "ADMM-based fast algorithm for multi-group multicast beamforming in large-scale wireless systems," *IEEE Trans. Commun.*, vol. 65, no. 6, pp. 2685–2698, Jun. 2017.

[32] M. Dai and B. Clerckx, "Hybrid precoding for physical layer multicasting," *IEEE Commun. Lett.*, vol. 20, no. 2, pp. 228–231, Feb. 2016.

[33] Ö. T. Demir and T. E. Tuncer, "Hybrid beamforming with two bit RF phase shifters in single group multicasting," in *Proc. IEEE Int. Conf. Acoust. Speech Signal Process. (ICASSP)*, Shanghai, China, Mar. 2016, pp. 3271–3275.

[34] J. Huang, Z. Cheng, E. Chen, and M. Tao, "Low-complexity hybrid analog/digital beamforming for multicast transmission in mmWave systems," in *Proc. IEEE Int. Conf. Commun. (ICC)*, Paris, France, May 2017, pp. 1–6.

[35] O. E. Ayach, R. W. Heath, Jr., S. Abu-Surra, S. Rajagopal, and Z. Pi, "The capacity optimality of beam steering in large millimeter wave MIMO systems," in *Proc. IEEE Workshop Signal Process. Adv. Wireless Commun. (SPAWC)*, Cesme, Turkey, Jun. 2012, pp. 100–104.

[36] Z. Xiang, M. Tao, and X. Wang, "Massive MIMO multicasting in noncooperative cellular networks," *IEEE J. Sel. Areas Commun.*, vol. 32, no. 6, pp. 1180–1193, Jun. 2014.

Zihuan Wang (S'17) received the B.S. degree in electronics information engineering from the Dalian University of Technology, Dalian, China, in 2017. She is currently pursuing the M.S. degree with the School of Information and Communication Engineering, University of Technology, Dalian.

Her current research interests include signal processing in massive MIMO and mmWave communications, multicast transmission, multiuser techniques, and cell-free architectures.

Qian Liu (S'09–M'14) received the B.S. and M.S. degrees from the Dalian University of Technology, Dalian, China, in 2006 and 2009, respectively, and the Ph.D. degree from the State University of New York at Buffalo (SUNY-Buffalo), Buffalo, NY, USA, in 2013.

She was a Post-Doctoral Fellow with Ubiquitous Multimedia Laboratory, SUNY-Buffalo from 2013 to 2015 and the Chair of Media Technology and the Chair of Communication Networks, Technical University of Munich from 2016 to 2017. She is currently an Associate Professor with the School of Computer Science and Technology, Dalian University of Technology. Her current research interests include multimedia transmission over MIMO systems, IEEE 802.11 wireless networks and LTE networks, device-to-device communication, energy-aware multimedia delivery, and the tactile Internet. She was a recipient of the Alexander von Humboldt Fellowship in 2015, and the Best Paper Runner-up Award at the 2012 IEEE International Conference on Multimedia and Expo and was in the Finalist for the Best Student Paper Award at the 2011 IEEE International Symposium on Circuits and Systems.

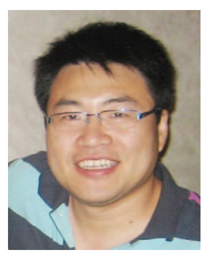

Ming Li (S'05–M'11–SM'17) received the M.S. and Ph.D. degrees in electrical engineering from the State University of New York at Buffalo (SUNY-Buffalo), Buffalo, in 2005 and 2010, respectively.

From 2011 to 2013, he was a Post-Doctoral Research Associate with the Signals, Communications, and Networking Research Group, Department of Electrical Engineering, SUNY-Buffalo. From 2013 to 2014, he joined Qualcomm Technologies, Inc., as a Senior Engineer. Since 2014, he has been with the School of Information and Communication Engineering, Dalian University of Technology, Dalian, China, where he is currently an Associate Professor. His current research interests are in the general areas of communication theory and signal processing with applications to mmWave communications, secure wireless communications, cognitive radios and networks, data hiding, and steganography.

Wolfgang Kellerer (S'96–A'02–M'03–SM'11) received the Dipl.-Ing. (master's) and Dr.-Ing. (Ph.D.) degrees from the Technical University of Munich, Germany, in 1995 and 2002, respectively, where he is a Full Professor, heading the Chair of Communication Networks with the Department of Electrical and Computer Engineering. He was with the European Research Laboratories of NTT DOCOMO for ten years in leading positions, contributing to research and standardization of LTE-A and 5G technologies. In 2001, he was a Visiting Researcher with Information Systems Laboratory, Stanford University, CA, USA. His research has resulted in over 200 publications and 35 granted patents. He was awarded with an ERC Consolidator Grant from the European Commission for his research project FlexNets Quantifying Flexibility in Communication Networks in 2015. He currently serves as an Associate Editor for the IEEE TRANSACTIONS ON NETWORK AND SERVICE MANAGEMENT and on the Editorial Boards for the IEEE COMMUNICATIONS SURVEYS & TUTORIALS and the IEEE NETWORKING LETTERS. He is a member of ACM and VDE ITG.